Polarization Relaxation in Triglycine Sulfate above the Curie Temperature

R. M. HILL AND S. K. ICHIKI
General Telephone and Electronics Laboratories, Inc., Microwave Physics Laboratory, Palo Alto, California
(Received June 18, 1962)

Measurements of the complex dielectric constant for normal and deuterated triglycine sulfate are reported. These measurements cover a range of 20°C above the Curie temperature and frequencies up to 7.7×10^{10} cps. A frequency- and temperature-dependent relaxation of the dielectric constant was observed which first sets in around 5×10^{7} cps. It was found that all the observations of ϵ^* could be expressed as

$$\epsilon^*=\frac{C}{T-T_c}[f(\nu\tau_0)+ig(\nu\tau_0)],$$

where C and T_c are the Curie constant and temperature; and τ_0 is inversely proportional to $(T-T_c)$. Expressions for $f(\nu\tau_0)$ and $g(\nu\tau_0)$ which give a good fit to the data were derived by assuming that each dipole has a Debye relaxation characteristic and that there is a Gaussian distribution of relaxation times, with τ_0 being the measure of the width of the distribution.

INTRODUCTION

THE dynamic properties of single-crystal ferroelectric materials below the Curie temperature have been studied in considerable detail,[1] because of possible technical applications of domain switching. The behavior of these materials in the paraelectric region, i.e., above the Curie temperature, has received less attention. Many approaches to an understanding of ferroelectricity above and below the Curie temperature, notably that of Devonshire,[2] have stressed equilibrium or static behavior, while the time dependence of the polarization has received less attention. Mason,[3] using a model of a dipole with two equilibrium positions acting under the influence of an average local field, has predicted a time dependence which has a single, Debye relaxation time proportional to $1/(T-T_c)$, where T_c is the Curie temperature. Akao and Sasaki[4] reported measurements made on Rochelle salt at frequencies up to 20 kMc/sec, which showed a relaxation frequency which decreased to a minimum of 2 kMc/sec at the Curie temperature. They interpreted these results in terms of Mason's theory, but were unable to fit their data above T_c by a single Debye relaxation time. In addition Lurio and Stern[5] have reported a set of measurements on triglycine sulfate (TGS) from 1 kc/sec to 2500 Mc/sec which indicates a relaxation onset between 100 and 500 Mc/sec.

Cochran[6] has recently proposed that a principal mechanism of ferroelectricity is the decrease in resonance frequency and resulting instability of one of the optically active lattice modes. He predicts that the frequency, ω_t, has a temperature dependence of $\omega_t\propto(T-T_c)^{1/2}$. Barker and Tinkham[7] have reported the presence of a broad, far infrared absorption in $SrTiO_3$, the peak frequency of which varies as $(T-T_c)^{1/2}$. Their data indicate that the strength of this absorption is sufficient to account for at least 95% of the low-frequency polarization. Measurements of the temperature dependence of the microwave loss tangent of $SrTiO_3$, by Rupprecht *et al.*,[8] were analyzed in terms of the Cochran model.

This paper reports measurements of the complex dielectric coefficient, ϵ^*, of normal and deuterated single-crystal triglycine sulfate, TGS, from 1 kc/sec to 77 kMc/sec, and from $T=T_c$ to T_c+20°C. In the frequency range studied the polarization relaxation is observed for temperatures near T_c. By using a Gaussian distribution of relaxation times, expressions for ϵ_1 and ϵ_2 are derived which fit the data quite well over the range of temperature and frequency studied.

EXPERIMENT

The determination of ϵ^* was made by three different techniques, each appropriate to a given frequency range. In the region from 1 kc/sec to 50 Mc/sec standard techniques for the measurement of capacity and circuit Q were applied. A thin, crystal slab with evaporated gold electrodes, was mounted inside a small cylindrical heating chamber. In this frequency range measurements were made as a function of dc bias, temperature, and ac level.

The sample holder used for frequencies from 500 to 5000 Mc/sec was similar to those used by numerous investigators.[9] However, a Teflon-filled 3/8-in. coaxial

[1] W. T. Merz, Phys. Rev. **95**, 690 (1954); R. C. Miller and A. Savage, *ibid.* **115**, 1176 (1959); A. G. Chynoweth and J. L. Abel, J. Appl. Phys. **30**, 1073 (1959).
[2] A. F. Devonshire, in *Advances in Physics*, edited by N. F. Mott (Taylor and Francis, Ltd., London, 1954), Vol. 3, p. 86.
[3] W. P. Mason, *Piezoelectric Crystals and Their Application in Ultrasonics* (D. Van Nostrand Company, Inc., Princeton, New Jersey, 1950), p. 234.
[4] H. Akao and T. Sasaki, J. Chem. Phys. **23**, 2210 (1955).
[5] A. Lurio and E. Stern, J. Appl. Phys. **31**, 1125 (1960).
[6] W. Cochran, in *Advances in Physics*, edited by N. F. Mott (Taylor and Francis, Ltd., London, 1960), Vol. 9, p. 387.
[7] A. S. Barker, Jr., and M. Tinkham, Phys. Rev. **125**, 1527 (1962).
[8] G. Rupprecht, R. O. Bell, and B. D. Silverman, Phys. Rev. **123**, 97 (1961).
[9] E. T. Janes and V. Varenhorst, Microwave Laboratory Report-287, Stanford University, Stanford, California (unpublished); E. Stern and A. Lurio, Phys. Rev. **123**, 117 (1961); O. B. Sharp and C. G. Brockus, Final Report 2732-4*F*, University of Michigan Research Institute, Ann Arbor, Michigan (unpublished).

line was used in place of the usual 7/8-in. line to extend the measurements to higher frequency, i.e., up to 6 kMc/sec. The sample holder consisted of a short section of 50-Ω coaxial line terminated by the crystal capacitor, whose dimensions were roughly 0.5×0.5×0.4 mm. A heater coil was wound on the sample holder and the entire assembly wrapped in insulating glass wool. The temperature of the sample was measured under equilibrium conditions by means of an iron-Constantan thermocouple.

The quantity measured with this apparatus is the complex impedance of the crystal. The impedance measurement of the crystal capacitor consists of observing the shift of the voltage standing-wave minimum with respect to a reference short and the magnitude of the voltage standing-wave ratio (VSWR) in a coaxial slotted line. These measurements are sufficient to determine the capacitance and the loss tangent of the sample if corrections for effects, such as the discontinuities in the slotted line and connectors, higher-order modes in the sample, and the end reactances of the sample holder, are taken into account. Since the discontinuities in the test line can shift the true position of the voltage null, a calibration procedure is necessary in order to correct this effect. Calibrations were made at each of the frequencies to be measured with a specially constructed adjustable short containing a section duplicating the geometry of the sample holder. The procedure is similar to the nodal shift technique for evaluating a very low reflection from a lossless coupling network. The other corrections, due to the line losses, higher-order modes in the crystal, and sample-holder end reactances are essentially similar to those described by Janes and Varenhorst[9]; a slight modification, however, is required when the measurements are extended into the higher frequency regions of 4 to 6 kMc/sec. Their method of evaluating the lumped circuit at the end region of the sample holder works satisfactorily below 2 to 3 kMc/sec, but at higher frequencies the small series inductance due to the reduced diameter of the crystal at the end region needs to be taken into account, particularly when the capacitance of the crystal is large enough to bring the current maximum near the end region. The inductive reactance term was evaluated experimentally by measuring the shift in the null position, with the end region terminated in a dummy metallic replica of the crystal sample, compared to the null position observed when the sample holder is terminated in a short circuit without the discontinuity.

In the high-frequency region (15 kMc/sec and above), the measurements were made on single-crystal windows mounted into sections of rectangular waveguide. Two waveguide sizes have been used: 0.280 in.×0.140 in. i.d. from 30 to 40 kMc/sec and 0.622 in.×0.211 in. i.d. from 15 to 20 kMc/sec. A measurement made by White and Tinkham[10] at 77 kMc/sec is included with our results.

[10] R. H. White and M. Tinkham (private communication).

The quantities measured in the high-frequency range are the power reflection and transmission coefficients. Since ϵ_1, the real part of the dielectric coefficient, is typically between 50 and 100 in this region, the reflection coefficient can be inconveniently large unless an impedance matching network is used. Small errors in the measurement will cause large changes in the inferred value of ϵ_1. To overcome this, quarter-wave transforming sections were placed on each side of the ferroelectric. The impedance Z_t of these sections was designed to be

$$Z_t^2 = Z_\omega Z_c, \tag{1}$$

where Z_ω is the waveguide impedance and Z_c is the impedance of the window section containing the crystal. When (1) holds the waveguide sections are matched.

Because Z_c varies markedly with temperatures it was necessary to have several sets of these matching sections corresponding to different impedances. They were made of Stycast $Hi-K$ dielectric.

Under nearly matched conditions the transmission coefficient is given by

$$T = (1-R_1)(1-R_2)\exp(-2\beta_2 d), \tag{2}$$

where $\beta_2 d$ is the product of the crystal phase constant times the thickness, and R_1 and R_2 are the reflection coefficient for the front and back interfaces between the crystal and the matching sections. Equation (2) assumes that only single reflections from these interfaces are important, a condition which holds over the frequency and temperature range studied by this technique. R_1 is measured for the section containing the transformer-crystal-transformer pieces, and then the entire assembly containing these pieces is reversed and the second reflection coefficient R_2 is measured.

A third set of measurements is made using the quarter-wave transformers only at the back face of the crystal. This approximates an infinitely long sample, for which the reflection coefficient is

$$R = \left|\frac{\gamma_1-\gamma_2}{\gamma_1+\gamma_2}\right|^2, \tag{3}$$

where $\gamma_1=\alpha_1+j\beta_1=(2\pi/\lambda)[1-(\nu_c/\nu)^2]^{1/2}$ is the propagation constant for the rectangular waveguide ($\beta_1=0$) and $\gamma_2=\alpha_2+j\beta_2=(2\pi/\lambda)[\epsilon^*-(\nu_c/\nu)^2]^{1/2}$ is the propagation constant for the waveguide section containing the crystal, and ϵ^* is the complex dielectric constant. For ferroelectric crystals $\epsilon_1 \gg (\nu_c/\nu)^2$ and $\gamma_2=(2\pi/\lambda)(n_1-jn_2)$, where n_1 and n_2 are the real and imaginary part of the index of refraction. The dielectric constants are then evaluated from

$$\epsilon_1 = n_1^2 - n_2^2, \quad \epsilon_2 = 2n_1 n_2, \tag{4}$$

where

$$n_1 = [1-(\nu_c/\nu)^2]^{1/2}\left\{\frac{1+R}{1-R}+\left[\left(\frac{1+R}{1-R}\right)^2 - \left(1+\frac{n_2^2}{1-(\nu_c/\nu)^2}\right)\right]^{1/2}\right\} \tag{5}$$

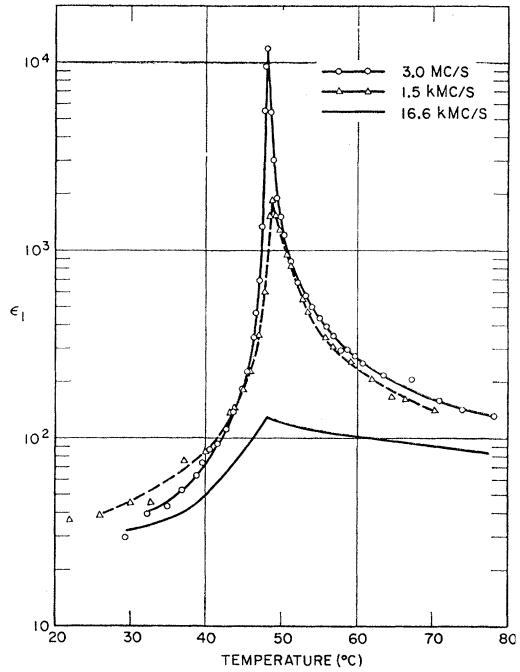

FIG. 1. Examples of data for ϵ_1, the real part of the dielectric constant, vs temperature in each frequency range.

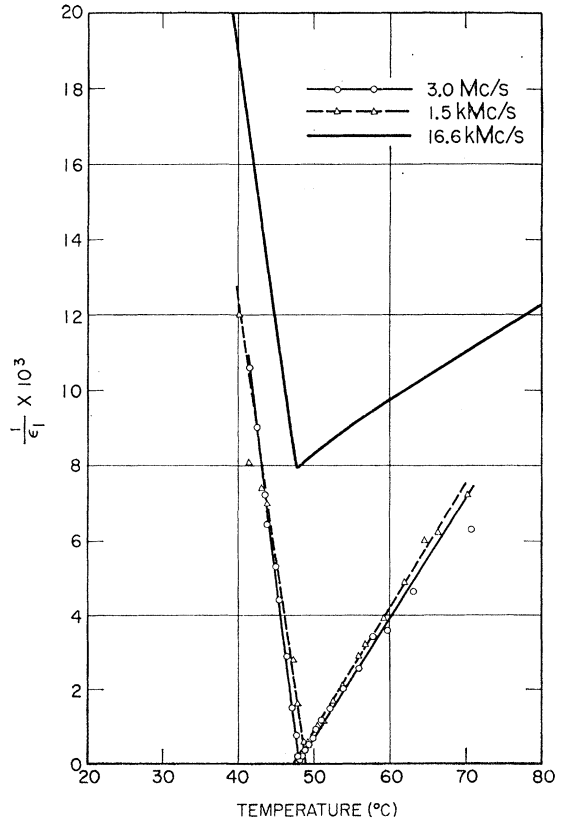

FIG. 2. Curie plots, $1/\epsilon_1$ vs T, for the data of Fig. 1.

and

$$n_2 = (\lambda/4\pi d) \ln[(1-R_1)(1-R_2)/T]. \quad (6)$$

The technique is susceptible to large errors when the dielectric constant to be measured is large and, therefore, the measurements must be made with great care. For example, measurement errors of 1% can lead to errors of 10 to 20% in the value of ϵ_1. This method is quite adequate for measurement on a lossy dielectric of medium (10 to 10^2) dielectric coefficient but on a low-loss dielectric, further refinements are necessary or other methods should be used.

RESULTS

Figure 1 shows typical plots of ϵ_1 vs temperature in each frequency range. Curie plots of the data in Fig. 1 are shown in Fig. 2. Table I gives the values of Curie constant C, Curie temperature T_c, both for the normal and deuterated TGS and loss constant α, defined below. No significant change in T_c was found in the frequency range covered. Determination of Devonshire's coefficients, A and B,[2] and values of the polarization P_s,

TABLE I. Paraelectric parameters for normal and deuterated triglycine sulfate.

	Curie constant C (°C)	Curie temperature T_c (°C)	Loss constant α [(kMc/sec)/°C]
TGS	3300	48.3	0.48
DTGS	4000	60.5	0.38

as a function of T, gave results in close agreement with those previously reported.[11]

All the data were taken at a given frequency as a function of temperature. Figure 3 shows these data replotted in terms of $\ln\epsilon_1$ vs $\ln\nu$ with $\Delta T = (T - T_c)$ as a parameter. Only data above T_c are used here and there was no external bias. There was a slight deviation in T_c from one apparatus to another. This is due to the different positions of the thermocouple with relation to the sample. Therefore, Fig. 3 has been plotted using the temperature for peak ϵ_1 as T_c.

Figure 3 reveals that ϵ_1 for each ΔT is asymptotic to a straight line of slope -1, implying a simple $1/\nu$ behavior at high frequencies. These data were then replotted in Fig. 4 using $\epsilon_1 \Delta T/C$ as the ordinate, where $C/\Delta T$ is the low-frequency value of ϵ_1, and $\nu/\alpha\Delta T$ as the abscissa, where α is a constant determined by matching the data for each T. Within the general spread of experimental points, ϵ_1 for all ΔT is seen to fall on a single curve. Setting $\tau_0 = 1/(\alpha\Delta T)$ we can see that $\epsilon_1 \Delta T/C$ can be represented by a single functional expression in terms of $\nu\tau_0$, where τ_0 is a "relaxation time,"

[11] S. Triebwasser, IBM J. Research Develop. 2, 212 (1958).

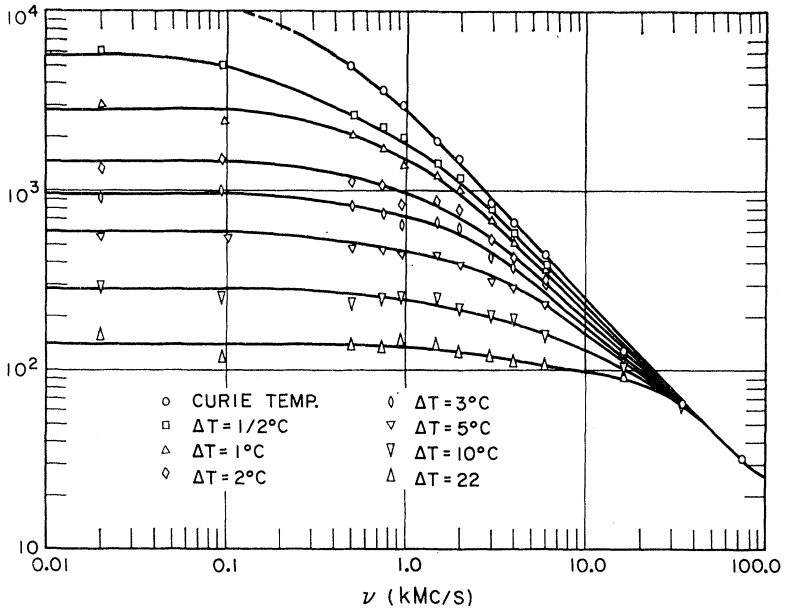

FIG. 3. ϵ_1 vs frequency ν, with $\Delta T = T - T_c$ as a parameter.

i.e.,

$$\epsilon_1 = [\epsilon_1(\nu=0)] f\left(\frac{\nu}{\alpha \Delta T}\right) = \frac{C}{T-T_c} f(\nu\tau_0). \qquad (7)$$

This leads to the interesting result that for TGS, only one parameter, α, in addition to C and T_c which are obtained at zero frequency, is needed to predict ϵ_1 at any frequency and temperature in the paraelectric region. α is determined by plotting the values of τ_0 for a best fit to the data as a function of ΔT and finding the slope. For TGS an $\alpha = 0.48$ (kMc/sec)/°C gives an excellent fit to the observed data. Figure 5 is a similar plot for the imaginary part ϵ_2, of thedielectric coefficient using the same value of α. These data show some spread, particularly around the maximum, which is indicative of the difficulty in measuring the loss accurately.

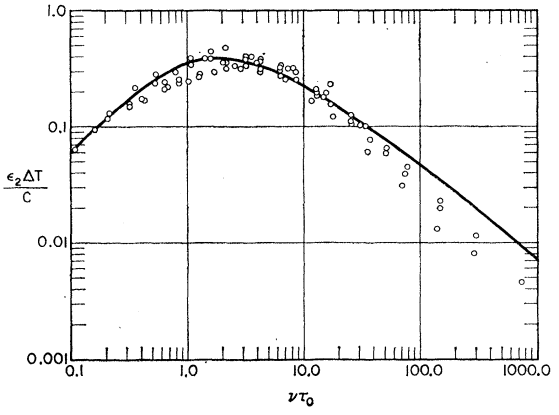

FIG. 5. ϵ_2 divided by $\epsilon_1(\nu=0)$ vs $\nu\tau_0$. The solid curve is derived as in Fig. 4. TGS.

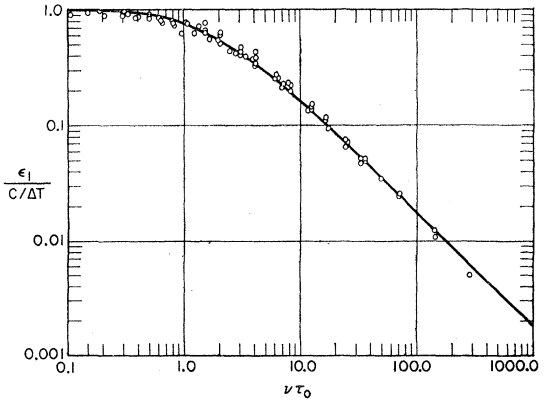

Fig. 4. ϵ_1 divided by $\epsilon_1(\nu=0)$ vs $\nu\tau_0$, where τ_0 has $\tau_0 = 1/\alpha(T-T_c)$ and α has been chosen for best fit. The solid curve is derived by assuming a distribution of Debye relaxation times. TGS.

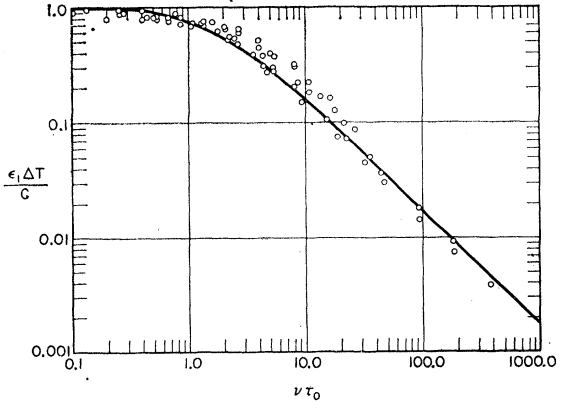

FIG. 6. ϵ_1, normalized by dividing by $\epsilon_1(\nu=0) = C/(T-T_c)$, vs the frequency ν. DTGS.

Figure 6 is a plot of the ϵ_1 data taken for the fully deuterated triglycine sulfate, DTGS, which had a T_c of 60.5°C. The form of the dependence on $(\nu\tau_0)$ is the same with an $\alpha=0.38$ (kMc/sec)/°C.

DISCUSSION

Figures 3 through 6 show that the complex dielectric coefficient of TGS can be represented as

$$\epsilon^*(\nu,\Delta T)=\epsilon_1(\nu=0)[f(\nu/\alpha\Delta T)+ig(\nu/\alpha\Delta T)]. \quad (8)$$

It is possible therefore to examine the frequency dependence of ϵ^* by studying only f and g which should be related to each other by the usual Kramers-Kronig relation. According to the usual Debye relation one would expect

$$\epsilon^*=\epsilon_1(\nu=0)\left(\frac{1}{1+(\nu\tau)^2}+\frac{i\nu\tau}{1+(\nu\tau)^2}\right). \quad (9)$$

This, of course, assumes a single time constant which characterizes all dipoles in the material. One observes that the measured dielectric coefficient for TGS is proportional to $1/\nu$ at high ν whereas according to the Debye relation it should be proportional to $1/\nu^2$. It is not at all surprising that a paraelectric material should deviate from simple Debye relaxation since it is not a "dilute" dipolar substance, i.e., the local field at a dipole can depend strongly on nearest-neighbor dipole orientations. However, we shall suppose that the dipoles behave like Debye dipoles but with a distribution of relaxation times. Let $y(\tau)$ be the distribution function; then one has

$$\epsilon_1-\epsilon_\infty=\int_0^\infty\frac{y(\tau)d\tau}{1+(\nu\tau)^2}, \quad (10)$$

$$\epsilon_2=\int_0^\infty\frac{\nu\tau y(\tau)d\tau}{1+(\nu\tau)^2}, \quad (11)$$

where $y(\tau)d\tau$ is the number of dipolar units having a relaxation time between τ and $\tau+d\tau$, per unit volume, subject to the zero frequency normalization

$$\int_0^\infty y(\tau)d\tau=\epsilon_1(\nu=0)=\frac{C}{T-T_c}. \quad (12)$$

If we let the distribution of relaxation times be Gaussian, i.e.,

$$y(\tau)=Ae^{-\tau^2/\tau_0^2},$$

where $\tau_0=1/[\alpha(T-T_c)]$, then (12) becomes

$$A\int_0^\infty e^{-\tau^2/\tau_0^2}d\tau=\frac{A}{2}\tau_0\sqrt{\pi}=\frac{C}{(T-T_c)}=\frac{A\sqrt{\pi}}{2\alpha(T-T_c)}. \quad (13)$$

This distribution then leads to a Curie-Weiss law for the zero-frequency behavior with $C=A\sqrt{\pi}/2\alpha$.

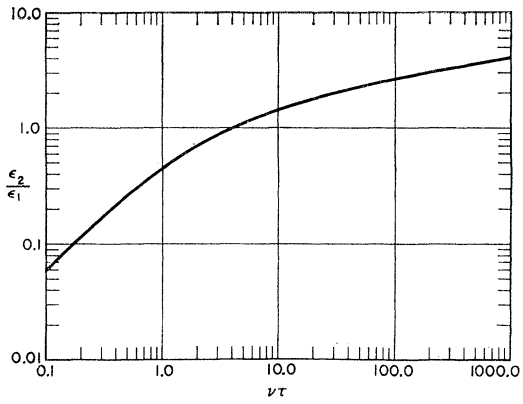

FIG. 7. Derived expression for ϵ_2 divided by the derived expression for ϵ_1 vs $\nu\tau_0$.

Equation (10) becomes

$$\epsilon_1-\epsilon_\infty=\frac{C}{\nu}\int_0^\infty\frac{e^{-x/(\nu\tau_0)^2}dx}{(1+x)x^{1/2}}, \quad (14)$$

where the substitution $x=(\nu\tau)^2$ has been made and $C=(A\sqrt{\pi})/2\alpha$.

The solution to (14) and the similar expression for ϵ_2 can be found in tables of Laplace transforms,[12] which give

$$\epsilon_1-\epsilon_\infty=\frac{C}{T-T_c}\pi^{1/2}\frac{1}{\nu\tau_0}e^{1/(\nu\tau_0)^2}\operatorname{erfc}(1/\nu\tau_0), \quad (15)$$

$$\epsilon_2=\frac{C}{T-T_c}\pi^{-1/2}\frac{1}{\nu\tau_0}e^{1/(\nu\tau_0)^2}[-\operatorname{Ei}(1/(\nu\tau_0)^2)], \quad (16)$$

where

$$\operatorname{erfc}(x)\equiv1-\operatorname{erf}(x)\equiv1-(2/\pi^{1/2})\int_0^x e^{-t^2}dt$$

and

$$-\operatorname{Ei}(-x)\equiv\operatorname{Ei}(x)\equiv\int_x^\infty\frac{e^{-t}dt}{t}.$$

The solid line given in Fig. 4 is a plot of Eq. (15), while Eq. (16) gives the solid line in Fig. 5. The expression for ϵ_1 is seen to fit the data quite well over several orders of magnitude change in ν and an order of magnitude in ΔT. The fit for ϵ_2 is fairly good up to $\nu\tau_0\simeq30$, although there is some spread around $\nu\tau_0=1$. Since ϵ_2 is considerably harder to measure, there is more scatter to the data. The deviation in ϵ_2 above $\nu\tau_0=30$ is unexplained. However, the Kramers-Kronig relation for ϵ_1 above $\nu\tau_0=10$ would not allow the observed ϵ_2. Figure 7 is a plot of the loss tangent, ϵ_2/ϵ_1, given by Eqs. (15) and (16). Again the data fit well up to $\nu\tau_0=30$.

We see that a "plausible" distribution of Debye dipoles can give a good fit to the data. We can only

[12] A. Erdlyi, W. Magnus, F. Oberhettinger, and F. Tricomi, *Tables of Integral Transforms* (McGraw-Hill Book Company, Inc., New York, 1954), p. 134.

speculate at this point as to what may give rise to this distribution. It seems reasonable to assume that the "relaxation time" of any given dipole is a function of the strength of the local field at that dipole and that for paraelectric materials, the local field is strongly dependent on the orientation of neighboring dipoles. The distribution of τ's would therefore arise from a distribution of clusters of different sizes where dipoles tend to have a particular orientation. Any given dipole, over a period of time, would have all the allowed relaxation periods. A knowledge of the distribution of τ's does not enable one to go directly to a statement of the distribution of clusters. This would require knowing the dependence of τ upon the local field as well as how the local field depends on the orientation of surrounding dipoles.

From Eq. (13), the "normalizing" constant A, is given as

$$A=2C\alpha/\sqrt{\pi}. \tag{17}$$

Substituting the C and α from Table I we see that $A(\mathrm{TGS})=1.77\times10^{12}$ cps and $A(\mathrm{DTGS})=1.70\times10^{12}$ cps or very nearly a constant. A has the dimensions of frequency and might be thought of as a maximum rate at which a single dipolar unit could reorient itself. Any fluctuations involving more than one dipole, or a dipole with a large, inhibiting, local field would occur at a slower rate.

We have seen that τ_0 is quite accurately proportional to $1/(T-T_c)$ for the range covered, T_c to $T_c+20°\mathrm{C}$. This can be related to Cochran's model by noting that the relaxation time for an overdamped, harmonic system is given by $\tau_0=\gamma/\omega_0^2$, where ω_0 is the resonant frequency of the undamped oscillator and γ is the damping constant. Cochran proposed that ω_0 for an optical mode of the crystal would behave as

$$\omega_0\propto(T-T_0)^{1/2}, \tag{18}$$

giving τ_0 proportional to $1/(T-T_0)$. It is less clear how to discuss a distribution of relaxation times in this case.

SUMMARY

We have shown that the dielectric constant for triglycine sulfate is given by an expression of the form

$$\epsilon^*=\frac{C}{T-T_c}\left[f\left(\frac{\nu}{\alpha(T-T_c)}\right)+ig\left(\frac{\nu}{\alpha(T-T_c)}\right)\right].$$

By assuming a Gaussian distribution of Debye relaxation times, expressions for f and g have been derived which are seen to fit the data well. Possible sources of this distribution, such as dipolar clustering, are discussed. Measurements underway on KD_2PO_4 may show whether this behavior is a general one.

ACKNOWLEDGMENTS

The authors wish to express their appreciation to Dr. G. Herrmann and Professor M. Tinkham for many helpful discussions and to D. Littfin for assistance in the measurements.